IAU Colloquium 190 on Magnetic Cataclysmic Variables
ASP Conference Series, Vol. 315, 2004
Sonja Vrielmann & Mark Cropper, eds.

The Fe XXII I(11.92 Å)/I(11.77 Å) Density Diagnostic

Christopher W. Mauche, Duane A. Liedahl, and Kevin B. Fournier

Lawrence Livermore National Laboratory,
L-473, 7000 East Avenue, Livermore, CA 94550

Abstract. Using the Livermore X-ray Spectral Synthesizer, which calculates spectral models of highly charged ions based on HULLAC atomic data, we investigate the temperature, density, and photoexcitation dependence of the $I(11.92\ \text{Å})/I(11.77\ \text{Å})$ line ratio of Fe XXII. Applied to the *Chandra* HETG spectrum of the intermediate polar EX Hya, we find that the electron density of its $T_{\rm e} \approx 12$ MK plasma is $\log n_{\rm e}\,({\rm cm}^{-3}) = 14.3^{+0.7}_{-0.5}$, orders of magnitude greater than that observed in the Sun or other late-type stars.

1. Introduction

The unique aspect of the high-temperature plasma in the post-shock region of the accretion flow of magnetic cataclysmic variables (mCVs) is its density, which is expected to be high because of the magnetic funneling of the mass lost by the secondary; the factor-of-four density jump across the accretion shock; and the settling nature of the post-shock flow, where the density scales inversely with the temperature. The standard density diagnostic of high-temperature plasmas is the intensity ratio $R \equiv f/i$ of the forbidden to intercombination lines of He-like ions, but this diagnostic is compromised in mCVs for two reasons (see Mauche 2002 for details). First, the critical density of this ratio increases with Z and hence temperature—the opposite of the trend in the accretion column—so the R line ratio is effective over only a narrow range of temperatures. Second, in mCVs and other UV-bright stars, photoexcitation competes with collisional excitation to depopulate the upper level of the forbidden line, so the R line ratio can appear to be in the "high-density limit" if the radiation field is sufficiently strong at the appropriate wavelengths. For example, in a plasma illuminated by a 30 kK blackbody, the R line ratios of all elements through Mg lie in the high-density limit, regardless of the density.

Recently, Mauche, Liedahl, & Fournier (2001, hereafter MLF) discussed the temperature, density, and photoexcitation sensitivity of the $I(17.10\ \text{Å})/I(17.05\ \text{Å})$ line ratio of Fe XVII. This line ratio is well suited to mCVs because its critical density is high ($n_{\rm c} \approx 3 \times 10^{13}$ cm^{-3}, comparable to that of Si XIII) and it is less sensitive to photoexcitation. Applied to the *Chandra* HETG spectrum of the intermediate polar EX Hya, MLF showed that the measured $I(17.10\ \text{Å})/I(17.05\ \text{Å})$ line ratio can be explained if the electron density $n_{\rm e} \gtrsim 2 \times 10^{14}$ cm^{-3}, or if the photoexcitation temperature $T_{\rm bb} \gtrsim 55$ kK.

https://doi.org/10.1017/S0252921100001949 Published online by Cambridge University Press

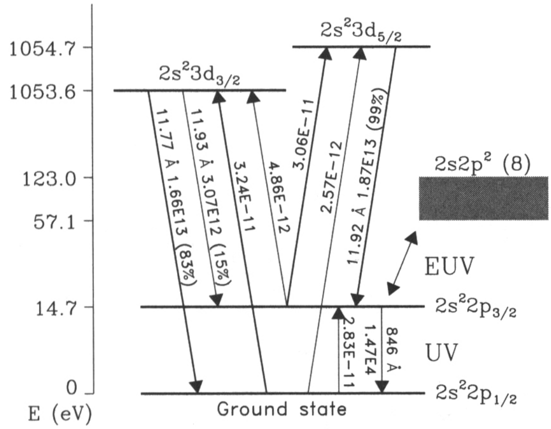

Figure 1. Schematic energy level diagram of Fe XXII showing the wavelengths, radiative decay rates, and branching ratios (*downward pointing arrows*) and collisional rate coefficients for T_e = 12.8 MK (*upward pointing arrows*) for the $2p$–$3d$ transitions. Population in the $2s^2 2p_{3/2}$ level is also built up through radiative cascades from the $2s2p^2$ manifold.

2. Fe XXII

Seeking to circumvent the density/photoexcitation ambiguity of the He-like R and Fe XVII $I(17.10\ \text{Å})/I(17.05\ \text{Å})$ line ratios, we undertook an investigation of the temperature, density, and photoexcitation dependence of the $3 \rightarrow 2$ transitions of Fe XXII (see Wargelin et al. 1998 for a discussion of the Fe XXII $4 \rightarrow 2$ transitions). Figure 1 shows a schematic of the important level-population processes in Fe XXII. The density sensitivity of the $n \rightarrow 2$ transitions of Fe XXII is due to the build-up of electron population in the first excited $2s^2 2p_{3/2}$ level due to the slow radiative decay rate out of that level, the 15% branching ratio from the $2s^2 3d_{3/2}$ level, and cascades through the $2s2p^2$ manifold. The population in the $2s^2 2p_{3/2}$ level is essentially unaffected by photoexcitation because the $2s^2 2p_{1/2}$–$2s^2 2p_{3/2}$ transition in the UV is not optically allowed, and the $2s^2 2p_{3/2}$–$2s2p^2$ transitions lie in the EUV, where observations (Hurwitz et al. 1997) demonstrate there is at most a weak source of continuum photons. The density sensitivity of the $3 \rightarrow 2$ transitions of Fe XXII manifests itself most clearly in the $I(11.92\ \text{Å})/I(11.77\ \text{Å})$ line ratio. This ratio is ~ 0.4 in low-density plasma (Brown et al. 2002), but is a factor of 2–3 times higher—1.06 ± 0.23—in the *Chandra* HETG spectrum of EX Hya (see Fig. 2).

To investigate the atomic kinetics of the $3 \rightarrow 2$ transitions of Fe XXII, we used the Livermore X-ray Spectral Synthesizer (LXSS), a suite of IDL codes that calculates spectral models of highly charged ions based on Hebrew University/Lawrence Livermore Atomic Code (HULLAC) atomic data. Our Fe XXII model includes radiative transition rates for E1, E2, M1, and M2 decays and electron impact excitation rate coefficients for levels with principal quantum

https://doi.org/10.1017/S0252921100001949 Published online by Cambridge University Press

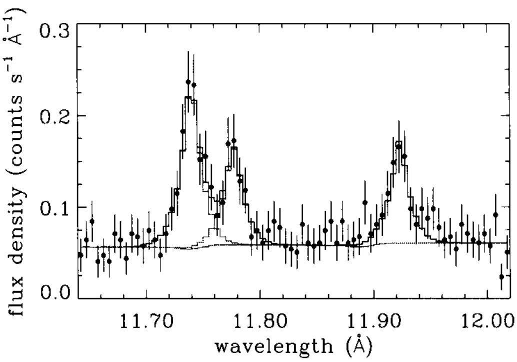

Figure 2. Detail of the *Chandra* MEG spectrum of EX Hya in the neighborhood of the Fe XXII $2p$–$3d$ lines. Data are shown by the filled circles with error bars and the model (3 Gaussians plus a linear background convolved with the HETG spectral resolution and effective area) is shown by the histograms. The line at 11.74 Å is due to Fe XXIII.

number $n \leq 5$ and azimuthal quantum number $l \leq 4$ for a total of 228 levels. To account for photoexcitation, we included in the LXSS population kinetics calculation the photoexcitation rates $(\pi e^2/m_e c) f_{ij} (4\pi/h\nu) B_\nu(T_{\rm bb})$, where $B_\nu(T_{\rm bb})$ is the blackbody spectral energy distribution and f_{ij} are the oscillator strengths of the various transitions. Using these data, LXSS calculates the level populations for a given temperature and density assuming collisional-radiative equilibrium; the line intensities are then simply the product of the level populations and the radiative decay rates (for details, see MLF).

Figure 3 shows the results of our calculations for the Fe XXII I(11.92 Å)/ I(11.77 Å) line ratio as a function of electron density for temperatures $T_{\rm e} = 6.3$, 12.8, and 25.5 MK. We find that this line ratio has a critical density $n_{\rm c} \approx 10^{14}$ cm^{-3}, is ≈ 0.3 at low densities and ≈ 1.4 at high densities, has only a very weak temperature dependence, and has only a weak photoexcitation dependence for blackbodies with temperatures $T_{\rm bb} \lesssim 60$ kK. Given the measured value of the I(11.92 Å)/I(11.77 Å) line ratio in EX Hya, we infer that the electron density of its $T_{\rm e} \approx 12$ MK plasma is $\log n_{\rm e}$ (cm^{-3}) $= 14.3^{+0.7}_{-0.5}$ (see Fig. 3).

3. Summary and Conclusions

To date, four spectroscopic diagnostics have provided evidence of high densities in the X-ray–emitting plasma of the intermediate polar EX Hya. Hurwitz et al. (1997) used the line ratio of the Fe XX/Fe XXIII 133 Å blend to the Fe XXI 129 Å line observed in the 1994 *EUVE* spectrum of EX Hya to infer $n_{\rm e} \gtrsim 10^{13}$ cm^{-3} for its $T_{\rm e} \approx 10$ MK plasma. Using the 2000 *Chandra* HETG spectrum of EX Hya, Mauche (2002) showed that the He-like R line ratios of O, Ne, Mg, Si, and S are all in their high-density limit; MLF used the Fe XVII I(17.10 Å)/I(17.05 Å) line ratio to infer $n_{\rm e} \gtrsim 2 \times 10^{14}$ cm^{-3} for its $T_{\rm e} \approx 4$ MK plasma; and we here used

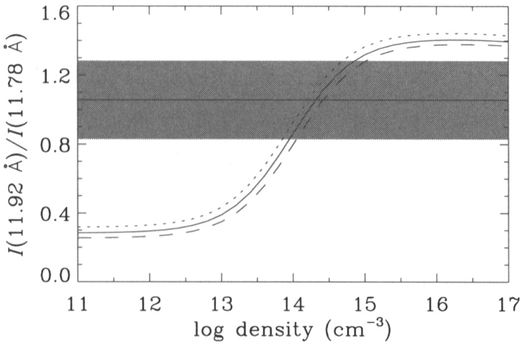

Figure 3. LXSS model of the Fe XXII $I(11.92\ \text{Å})/I(11.77\ \text{Å})$ line ratio as a function of electron density for temperatures $T_e = 6.3$, 12.8, and 25.5 MK (*dotted, solid, and dashed curves, respectively*). The horizontal line and shaded stripe indicate the value and $1\,\sigma$ error envelope of the line ratio measured in EX Hya.

the Fe XXII $I(11.92\ \text{Å})/I(11.77\ \text{Å})$ line ratio to infer $n_e \approx 2 \times 10^{14}$ cm^{-3} for its $T_e \approx 12$ MK plasma. Of these diagnostics, the Fe XVII and Fe XXII line ratios are the most reliable, with the Fe XXII diagnostic limited only by the quality of the data. We conclude first that the *Chandra* HETG spectrum of EX Hya requires plasma densities that are orders of magnitude greater than those observed in the Sun or other late-type stars, and second that the Fe XVII $I(17.10\ \text{Å})/I(17.05\ \text{Å})$ and (better still) the Fe XXII $I(11.92\ \text{Å})/I(11.77\ \text{Å})$ line ratios provide density diagnostics that are useful for sources like mCVs in which the plasma densities are high and the efficacy of the He-like density diagnostics is compromised by the presence of a bright UV continuum.

Acknowledgments. We thank H. Tananbaum for the generous grant of Director's Discretionary Time that made possible the *Chandra* observations of EX Hya. Support for this work was provided in part by NASA through *Chandra* Award Number DD0-1004B. This work was performed under the auspices of the U.S. Department of Energy by University of California Lawrence Livermore National Laboratory under contract No. W-7405-Eng-48.

References

Brown, G.V., Beiersdorfer, P., Liedahl, D.A., Widmann, K., Kahn, S.M., & Clothiaux, E.J. 2002, ApJS, 140, 589

Hurwitz, M., Sirk, M., Bowyer, S., & Ko, Y.-K. 1997, ApJ, 477, 390

Mauche, C.W., Liedahl, D.A., & Fournier, K.B. 2001, ApJ, 560, 992, MLF

Mauche, C.W. 2002, in The Physics of Cataclysmic Variables and Related Objects, ed. B.T. Gänsicke, K. Beuermann, & K. Reinsch (San Francisco: ASP), 113

Wargelin, B.J., Beiersdorfer, P., Liedahl, D.A., Kahn, S.M., & von Goeler, S. 1998, ApJ, 496, 1031